Supramolecular Strategy Based on Conjugated Polymers for Discrimination of Virus and Pathogens

Haotian Bai, Huan Lu, Xuancheng Fu, Endong Zhang, Fengting Lv, Libing Liu, and Shu Wang

Biomacromolecules, **Just Accepted Manuscript** • DOI: 10.1021/acs.biomac.8b00336 • Publication Date (Web): 10 Apr 2018

Supramolecular Strategy Based on Conjugated Polymers for Discrimination of Virus and Pathogens

Haotian Bai, Huan Lu, Xuancheng Fu, Endong Zhang, Fengting Lv, Libing Liu, Shu Wang**

Beijing National Laboratory of Molecular Science, Key Laboratory of Organic Solids, Institute of Chemistry, Chinese Academy of Sciences, Beijing 100910, P. R. China

Keywords: conjugated polymers, supramolecular strategy, biosensor, virus, pathogen

Abstract: A conjugated polymer-based supramolecular system is designed for discrimination of virus and microbes. The supramolecular system is composed of cationic polythiophene derivative (PT) and barrel-shaped macrocyclic molecular cucurbit[7]uril (CB[7]). Because PT and PT/CB[7] complex possess different interaction manners toward virus and microbes, the rapid and simple discrimination of virus and microbes was realized through polymer fluorescence intensity change assisting with standard linear discriminant analysis (LDA). The supramolecular strategy would expand the idea of designing biological probes, and further promote the extensive application of conjugated polymer materials in biosensor field.

1. Introduction

The public who are constantly and inevitably infected by pathogens, viruses and parasites, have not kept calm facing of these scientific data that exploded to popular media about the close connection between the abuse/misuse antibiotics and the spread antibiotic-resistance.[1-5] In both human medicine and agriculture-agrifood industry,[6,7] the diagnosis and discrimination of lethal infections caused by bacteria or virus play critical roles in appropriate use of germicides, however it is difficult even for experienced doctors and academics.[8-10] The aforemetntioned factors led to unnecessary treatments with antibiotics and the ever-increasing antibiotic resistance eventually.[11] Based on the data from World Health Organization (WHO) of 71 countries, totally global antibiotic consumption grew from 50 billion to 70 billion standard units (more than 30%) in the first decade of the 21st century.[12] And the American Center for Disease Control and Prevention (CDC) predicted that antibiotic-resistant infections would kill 10 million people worldwide by 2050.[13] Except for the inappropriate use in medical care, the recommended levels of antibiotics for feed in agricultural practices have risen 10-20 fold since 1950s due to the overuse and misuse of bactericides.[7, 14] And more concerning than the fact is that the rising multidrug-resistant pathogens have entered the human environments from animals rapidly, and they could easily travel through contacting with the air, water and contaminated food.[14-17] As illustrated that the enzyme linked immunosorbent assay (ELISA), polymerase chain reaction (PCR) and reverse-transcription polymerase chain reaction (RT-PCR) have been studied and applied in routine laboratory and clinical diagnosis, and the isolated culture combining with immunofluorescence (IF) is the "gold standard" for the detection and discrimination of pathogens and viruses, however, the complicated operations and expensive instruments restrict their popularization and applications.[18-23] Consequently, it is necessary to introduce innovative

materials and strategies, which can be utilized for detecting and differentiating of pathogens and viruses, for using the antibiotics properly and blocking the epidemic antibiotic-resistance.

Conjugated polymers have been employed for the detection and diagnosis of chemical and biological molecular due to their outstanding light harvesting and optical signal amplification effects.[24-26] Herein, we designed and constructed a supramolecular conjugated sensor based on a cationic polythiophene derivative (PT) and barrel-shaped macrocyclic molecular cucurbit[7]uril (CB[7]). Furthermore, we successfully realized the detection and discrimination virus and pathogens utilizing the supramolecular conjugated sensor.

2. Experimental Section

2.1 Materials and measurements. In the experiments, all chemicals and organic solvents were purchased from Sigma-aldrich Chemical Company, Alfa-Aesar and Beijing Chemical Works, and were used as received without further purification. The conjugated polymer (PT) was synthesized according to the published reports in our lab. TMV was kindly provided by Professor Wenke Zhang (Jilin University). All the microbial pathogens were purchased from Institute of Microbiology Chinese Academy of Sciences and resuscitated using standard processes. Black 96-well plate was purchased from Thermo Scientific. The ^{1}H NMR spectra were obtained using Bruker AVIII400WB apparatus. Dynamic light scattering (DLS) was measured on a Nano ZS90 (Malvern, UK). UV-Vis absorption measurements and the concentration of microorganisms were measured on a JASCO V-550 spectrophotometer. Fluorescence spectra were obtained from a Hitachi F-4500 fluorometer equipped with a xenon lamp as excitation source. The absolute fluorescence quantum yield (QY) was determined by a Hamamatusu absolute PL quantum yield

spectrometer C11347. Fluorescence intensity values for LDA analysis (performed by SPSS v20.0) were obtained on a microplate reader (BIO-TEK Synergy HT) using black 96-well plates.

2.2 Prepare of microbial analytes. A single colony of Amp^r *E. coli* (Top 10) on a solid agar plate of Luria-Bertani (LB) was transferred to 10 mL liquid LB culture medium and added 50 μg/mL ampicillin, and cultured at 37°C for 8 hours. As for *S. aureus* (ATCC6538) and *C. albicans* (CA10231), the culture medium was respectively replaced by Nutrient Broth (NB) and Yeast-extract Peptone Dextrose (YPD) without ampicillin. And *S. aureus* was cultured at 37°C for 8 hours as well, while *C. albicans* was grown at 30 °C for 12 h. Microbes were treated according to the following operations: Microbes were harvested by centrifuging (7100 rpm for 2 min) and they were washed with 1×PBS (10 mM, pH = 7.4) twice. The supernatant was discarded in each stage, and the remaining samples were suspended in PBS. The bacterial fluid of *E. coli* and *S. aureus* were diluted to an optical density of 1.0 at 600 nm (OD_{600}=1.0), and the fungi fluid of *C. albicans* were 2.0 OD_{600}. All the microbial fluid would be diluted according to the experimental need during the discriminated peocedures.

2.3 Isothermal titration microcalorimetry. ITC experiments were measured on a MicroCal ITC200 in phosphate buffer saline (PBS, 10 mM, pH = 7.4) at 298.15 ± 0.01 K. The data were processed by the software of NanoAnalyze and OriginPro 9.2. The thermodymanic parameters were obtained though fitting the ITC curves by using the model for single set of identical binding sites. The experiments were repeated at least twice with deviation within ±4%. The number of microorganisms was detected by counting the colony forming units (CFU) in standard plate

count experiments. The number of TMV was calculated as the weight-average molar mass (Mw = 4×10^4 KDa).

2.4 Fluorescence response for LDA. PT and PT/CB[7] were prepared with hyperpure water puried by Milli-Q^{TM} Advantage A10^{TM}, and the concentration of PT and PT/CB[7] is 200 μM. The total volume of black 96-well plate was 100 μL in each well, which include 10 μL fluorescence sensors, 20 μL of the tested samples, and 70 μL of 1×PBS. For the experimental group of different concentration analytes, 10 μL fluorescence sensors, 15 μL of the tested samples, and 75 μL of 1×PBS were used. The blank group contained only 1×PBS, and the control group contained 1×PBS and fluorescent sensors. Fluorescence data were collected on fluorescence plate reader after culturing 37°C for 25min.

3. Results and discussion

As exhibited in Scheme 1, our identification strategy only relied on the fluorescent signal feedback of PT and PT/CB[7] upon addition of analytes and standard linear discriminant analysis (LDA). LDA is a generalization of Fisher's linear discriminant, which has been extensively used in pattern recognition.[27] Not only is our method simple, rapid, accurate and reliable, but also it can greatly simplifies required process and steps of chemical synthesis. This work has combined the conjugated polymer materials in an elegantly optical manner with supramolecular chemistry for opening new avenues for bioanalysis and solving antibiotic resistance.

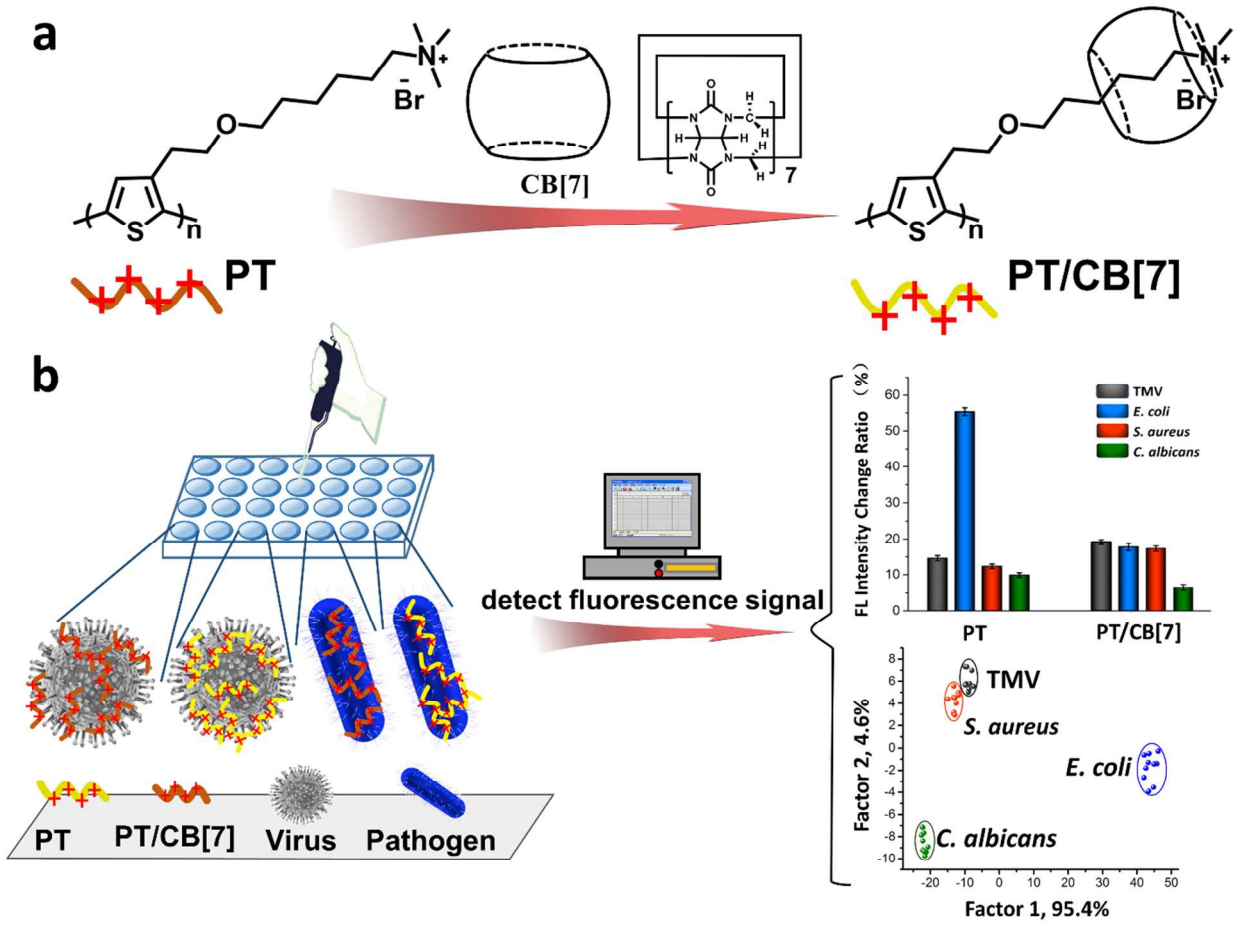

Scheme 1. (a) The preparation of supramolecular sensor system. (b) Schematic illustration of supramolecular sensor for detection and discrimination between virus and pathogens.

Firstly, we constructed and characterized the formation of the supramolecular host-guest complex between PT and CB[7]. PT was synthesized as the published synthesis process.[28] ^{1}H NMR experiments and isothermal titration calorimetry (ITC) were employed to investigate the structural properties, molecular interactions, thermodynamical process and interactive mechanism. As shown in Figure 1a, the peaks of protons on PT before and after complexation with CB[7] have been assigned correspondingly. Upon the addition of CB[7] to PT D_2O solution,

all the protons of PT displayed significant field shifts. The peaks related to protons b-g shifted to high magnetic field significantly after adding CB[7] (c-f: from 1.6 -1.0 ppm to 1.2-0.6 ppm; b, g: from 3.2-2.4 ppm to 2.7-2.1 ppm), while the peaks of h, i shifted to low magnetic field (from 3.2-2.4 to 3.7-3.2 ppm). It also should be noted that the characteristic peak of the protons in PT backbone (8.5–8.0 ppm) in D_2O appeared clearly upon binding CB[7]. CB[7] as a kind of barrel-shaped macrocyclic hosts, possessed a hydrophobic cavity and hydrophilic exterior. Thus, it could noncovalently attach to the QA side linkage of PT by the synergistic reaction of ion–dipole interactions, hydrogen bonds, and the hydrophobic effect. These observations demonstrated the formation of PT/CB[7] complex. And then, during the ITC experiments, it was titrated with standard solution CB[7] in PT supporting electrolyte. The binding affinity constant between CB[7] and PT was 5.1×10^6 M^{-1} (Figure 1b), which was calculated by fitting the ITC curve with one set of site binding model. And it could guarantee the stability and practicability of the supramolecular detecting sensor in the following experiments. Dynamic light scattering (DLS) was carried out to illustrate the aggregate size change of PT after encapsulation by CB[7]. As shown in Figure S2(a) and S2(b), the average diameter of PT enlarged significantly from 140 ± 2 nm to 185 ± 1 nm with narrower size distribution (Polydispersed index（PDI）from 0.28 to 0.45), which suggested that the bulky CB[7] could reduce the aggregation of PT and make the conjugated polymers better dispersity. The photophysical characterizations of PT and PT/CB[7] were the major factors, which would be employed in the following biological tests of detection and discrimination, UV/Vis absorption absorbance spectra and fluorescence spectra were collected. As Figure 1(c) and 1(d) illustrated, compared with the original PT, both the UV/Vis absorbance and fluorescence intensity increased evidently accompanying with a blue shift. The absolute fluorescence quantum yield (QY) of PT and PT/CB[7] were 4.9% and 5.6%,

respectively. It could be envisaged that, after encapsulation, the close stacking of hydrophobic conjugated backbones were impeded effectively by the bulky and space-demanding CB[7] molecules. The phenomena and results of optical physics explained the narrower size distribution of PT/CB[7] as well. In conclusion, all the above data and results verified that the supramolecular sensor PT/CB[7] was successfully formed and it would have potential to be applied in the following biological experiments.

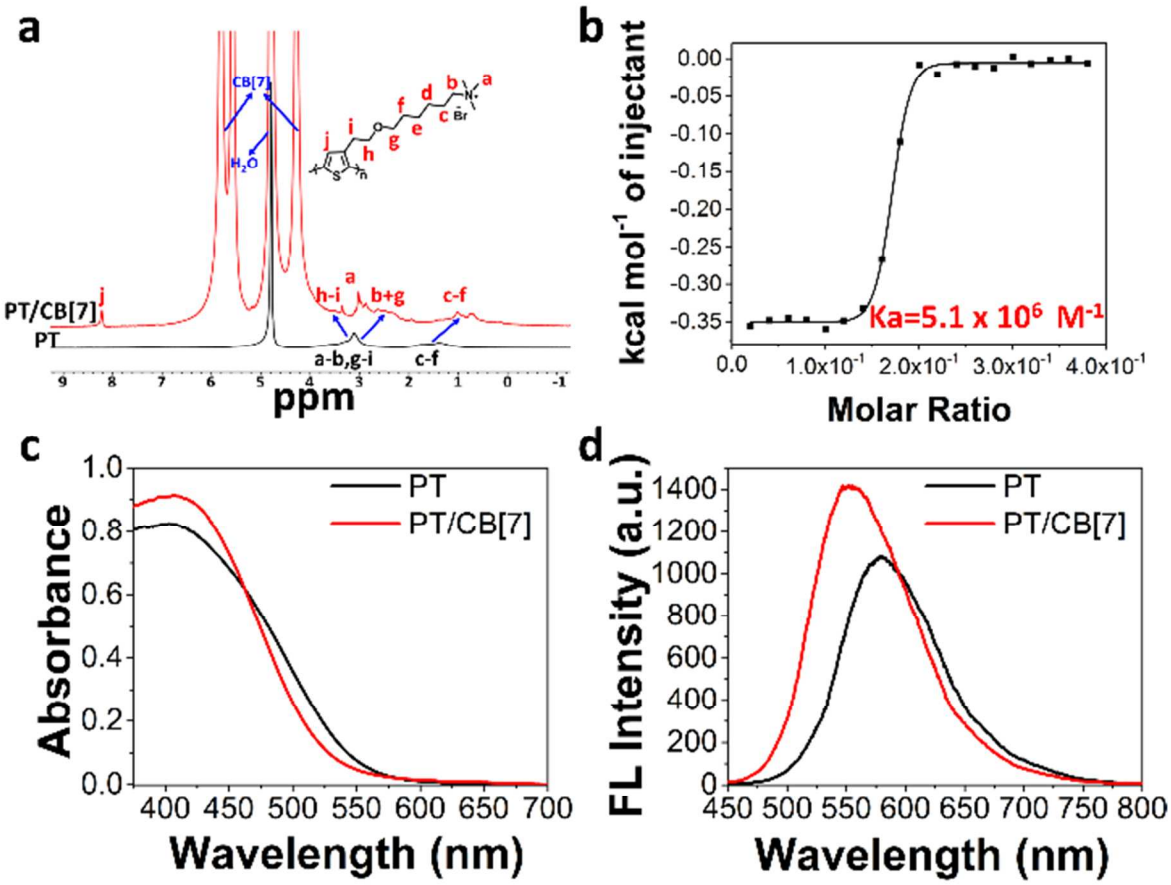

Figure 1. (a) ^{1}H NMR spectra of the PT and PT/CB[7] complex in D_2O, and the blue arrows indicate the peak shifts of the protons after adding CB[7]. (b) ITC fitting data and the binding constant of the host-guest complexation between CB[7] (Top) and PT. (c) UV−vis absorption spectra of PT and PT/CB[7] complex. (d) fluorescence spectra of PT and PT/CB[7] complex.

The concentration of PT in c, d is 0.2 mM in repeat units (RUs), and the concentration ratio of CB[7] and PT is 10.

According to the published reports, the cationic conjugated polymers binding with and without CB[7] both could intact and sting into microbial membrane, which would reduce the aggregation and decrease the self-quenching of conjugated polymers in aqueous solution.[29] It means that the various size, shape and surface status of pathogens and virus[30] could augment the diversity in the fluorescence response patterns of fluorescent sensor. Thus, we speculated that the two fluorescent sensors of PT and PT/CB[7] would have corresponding response signal, after they bound with different virus and microorganisms. Also isothermal titration microcalorimetry (ITC), which could visualize the thermodynamical process and interactive mechanism between texted samples and fluorescence sensors, was utilized for indicating the interaction between them. Tobacco mosaic virus (TMV) was selected to represent virus, and *E. coli*, *S. aureus* and *C. albicans* were chosen as the representative for gram-negative bacteria, gram-positive bacteria and fungi respectively. As shown in Figure 2, during the interaction process, with the dropping of PT and PT/CB[7], variations of observed enthalpy changes (ΔHobs) in all the texted samples were detected. It directly indicated that both of PT and PT/CB[7] could bind with these biological samples and all the interaction processes were an exothermic process undoubtedly. Furthermore, positively charged PT, as a typical amphiphile, could bind to negatively charged biosurface on the basis of the electrostatic and hydrophobic synergistic reaction.[24] PT/CB[7] was more inclined to interact with negatively charged biosurface through electrostatic process, because the CB[7] had encapsulated and prevented the alkyl side chains inserting driven by hydrophobic effect. It has been recognized that the surfaces of TMV, bacteria and fungi are all

negatively charged, but their surface structures are totally different. TMV consists of 2130 molecules of coat protein, and the coat protein self-assembles into the rod-like helical structure around the cored RNA.[31] The envelope of gram-negative bacterita (*E. coli*) consist of lipopolysaccharide trimer and protein, while that of gram-positive bacteria (*S. aureus*) consists of peptidoglycan, teichuronic acid and lipoteichoic acid. And fungi (*C. albicans*) possess an out layer of mannatide.[24] For the exothermic enthalpy is contributed by the electrostatic interaction,[32] the different values of ΔHobs can be utilized for researching the different electrostatic binding ability of PT and PT/CB[7] toward different kinds of biological samples, which have characteristic size, shape and membrane structure. The binding constant and combined ratio descripted the binding ability and binding numbers of PT and PT/CB[7] molecules associated with a single TMV, *E. coli*, *S. aureus* and *C. albicans*. Specifically, PT/CB[7] had stronger binding ability and large binding molecular amount toward TMV compared with PT, while PT also had large binding constant toward *S. aureus* and *C. albicans* compared with PT/CB[7], the combined ratios of PT/CB[7] toward them was less than that of PT. Although PT and PT/CB[7] had almost the same binding ability toward *E. coli*, the combined ratio were significantly different. It has been verified that conjugated polymer carrying quaternary ammonium groups could detect and discriminate microorganism possessing different surface structures.[24,33,34] Moreover, supramolecular conjugated polymer materials have different optical signal on the surface of pathogens before and after dis-assembly.[29] Therefore, two fluorescent sensors of PT and PT/CB[7], which have characteristic interaction ability with biological surface, offer great potential for biological detection and discrimination.

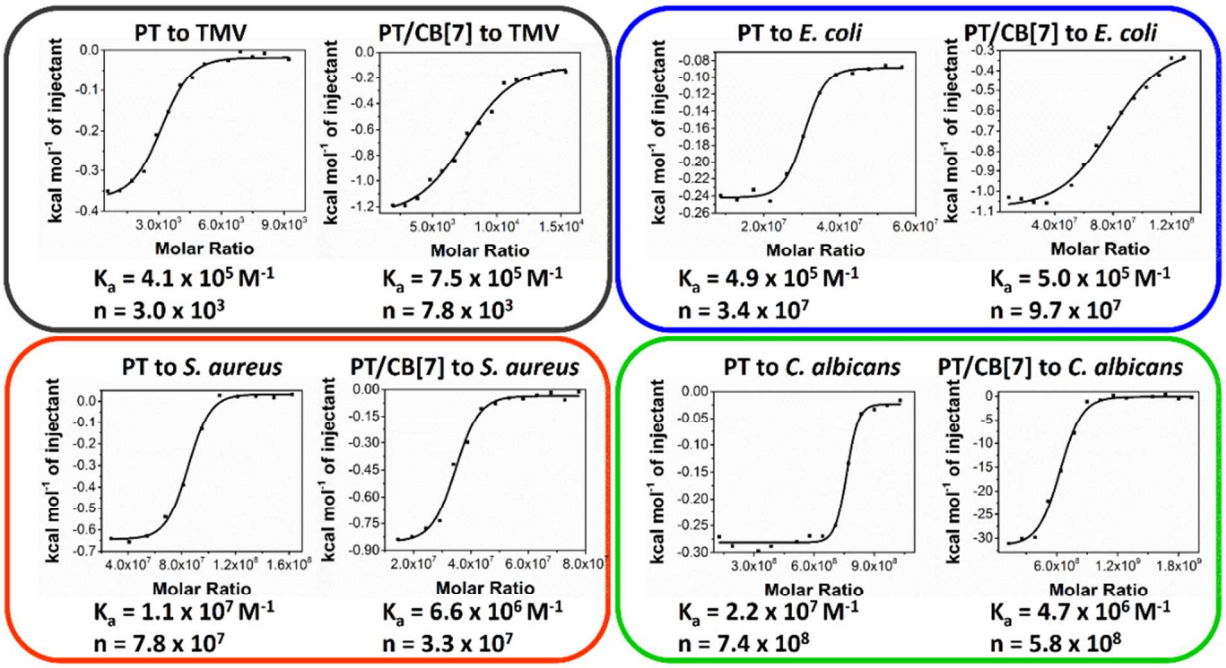

Figure 2. Fitting curves of thermodynamical changes of tested samples upon adding PT and PT/CB[7]. The standard dilution enthalpies of PT and PT/CB[7] in each independent experiments have been deducted.

Next, the fluorescence signals of two fluorescent sensors (PT and PT/CB[7]) upon addition of certain concentration of tested samples were collected. As expected, all the independent experiments directly exhibited that the fluorescence intensity of sensors increased after they interacted with both virus and microorganisms, shown in Figure 3 (a). Moreover, two concentrations of each tested sample demonstrated a similar tendency toward fluorescent change after the same experimental process. By calculating, in the experimental concentration range, the degree of fluorescence intensity almost unchanged. As the column diagram shown in Figure 3a, all tested samples had specific fluorescence intensity change ratio. For example, the fluorescence intensity change ratio of *E. coli* treated with PT had an increase of more than 50%, while that of

C. albicans treated with PT/CB[7] had a growth of less than 10%. Therefore, both PT and PT/CB[7] could implement characteristic fluorescence fingerprints for TMV, *E. coli*, *S. aureus* and *C. albicans*. Last, LDA was utilized to interprete the two-dimensional sensor data of each independent and parallel experiment. As shown in Figure 3b, LDA classified all the tested samples into four distinct clusters, corresponding to the different classifications and categories. Moreover, all the tested sample were well-clustered with 99.9% discriminating accuracy, and the two canonical scores carried about 95.4% and 4.6% of total variance. Above all, we eventually achieve the method of detection and discrimination between virus and microorganisms through the simple fluorescent response and LDA.

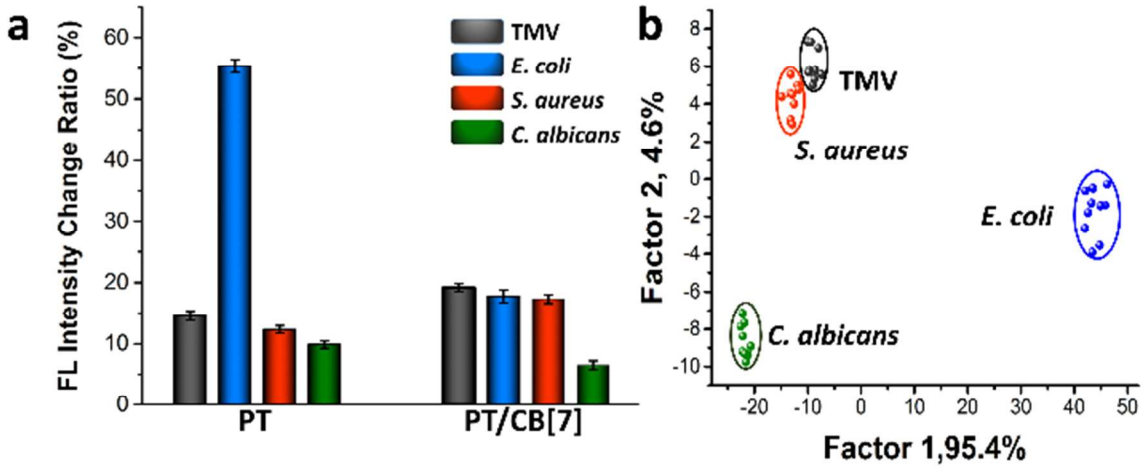

Figure 3. (a) The histogram of fluorescence response according to the fluorescence intensity, Fluorescence intensity of PT, PT/CB[7] and different microorganisms and virus treated with PT and PT/CB[7] for 25 min recorded by fluorescence plate reader. [PT] = 20 μM in RUs, [PT/CB[7]] = 20 μM in RUs, [TMV] = 0.2 mg/mL and 0.15 mg/mL, [*E. coli*] = 1.0×10^8 cfu/mL and 7.5×10^7 cfu/mL, [*S. aureus*] = 1.2×10^8 cfu/mL and 9×10^7 cfu/mL, [*C. albicans*] = 5×10^7

cfu/mL and 4×10^7 cfu/mL. ex = 430/30 nm, ex = 540/25 nm. (b) Clustering the tested TMV, *E. coli*, *S. aureus* and *C. albicans* via LDA of the fluorescent signal.

4. Conclusion

In summary, we have designed and constructed a simple and exact strategy for virus and pathogens identification and discrimination based on fluorescence signal response of PT and PT/CB[7]. The characteristic interaction ability of PT and PT/CB[7] with biological surfaces gave rise to specific fluorescence intensity change ratio of tested samples. After LDA interpreting the two-dimensional data of fluorescence intensity change ratio, the distinction of virus and pathogens was realized. Revolutionary supramolecular strategy decreased the essential synthesis steps of fluorescence sensor, and this work provided a simple, effective and rapid method for bioanalysis, which would contribute to intelligent use of antibiotics and combat against antibiotic resistance. What's more, it opens a new view of the application of supramolecular materials in the future, and we believe it will have a long-term impact on existing designed system of fluorescence probes.

ASSOCIATED CONTENT

Supporting Information. Additional Figures S1-S3. This material is available free of charge via the Internet at http://pubs.acs.org/.

Supplementary Figure S1. The molecular structure of CB[7]. Supplementary Figure S2 Size distribution histograms of PT and PT/CB[7]. Supplementary Figure S3, Fluorescence intensity of

PT, PT/CB[7] and different microorganisms and virus treated with PT and PT/CB[7] for 25 min recorded by fluorescence plate reader.

AUTHOR INFORMATION

Corresponding Author

*Email: wangshu@iccas.ac.cn (S.W.), lvft@iccas.ac.cn (F. L.)

Author Contributions

The manuscript was written through contributions of all authors. All authors have given approval to the final version of the manuscript.

Funding Sources

The National Natural Science Foundation of China and the Strategic Priority Research Program of the Chinese Academy of Sciences

Acknowledgements

The authors are grateful to the National Natural Science Foundation of China (Nos. 21533012, 21473221, 91527306, and 21661132006), the Strategic Priority Research Program of the Chinese Academy of Sciences (XDA09030306). We thank Professor Wenke Zhang (Jilin University) for kindly providing the TMV.

References

1 Berendonk, T. U.; Manaia, C. M.; Merlin, C.; Fatta-Kassinos, D.; Cytryn, E.; Walsh, F.; Burgmann, H.; Sorum, H.; Norstrom, M.; Pons, M. N.; Kreuzinger, N.; Huovinen, P.; Stefani, S.; Schwartz, T.; Kisand, V.; Baquero, F.; Martinez, J. L. Tackling antibiotic

resistance: the environmental framework. *Nat. Rev. Microbiol.* **2015,** *13*, 310-317.

2 Bush, K.; Courvalin, P.; Dantas, G.; Davies, J.; Eisenstein, B.; Huovinen, P.; Jacoby, G. A.; Kishony, R.; Kreiswirth, B. N.; Kutter, E.; Lerner, S. A.; Levy, S.; Lewis, K.; Lomovskaya, O.; Miller, J. H.; Mobashery, S.; Piddock, L. J. V.; Projan, S.; Thomas, C. M.; Tomasz, A.; Tulkens, P. M.; Walsh, T. R.; Watson, J. D.; Witkowski, J.; Witte, W.; Wright, G.; Yeh, P.; Zgurskaya, H. I. Tackling antibiotic resistance. *Nat. Rev. Microbiol.* **2011,** *9*, 894-896.

3 Nathan, C.; Cars, O. Antibiotic resistance - problems, progress, and prospects. *New Engl. J. Med.* **2014,** *371*, 1761-1763.

4 The antibiotic alarm. *Nature* **2013,** *495*, 141.

5 Ling, L. L.; Schneider, T.; Peoples, A. J.; Spoering, A. L.; Engels, I.; Conlon, B. P.; Mueller, A.; Schaberle, T. F.; Hughes, D. E.; Epstein, S.; Jones, M.; Lazarides, L.; Steadman, V. A.; Cohen, D. R.; Felix, C. R.; Fetterman, K. A.; Millett, W. P.; Nitti, A. G.; Zullo, A. M.; Chen, C.; Lewis, K. A new antibiotic kills pathogens without detectable resistance. *Nature* **2015,** *517*, 455-459 .

6 Antibiotic threat. *Nature* **2013,** *499*, 379.

7 Mole, B. Farming up Trouble. *Nature* **2013,** *499*, 398-400.

8 Kolakofsky, D. Paramyxovirus RNA synthesis, mRNA editing, and genome hexamer phase: A review. *Virology* **2016,** *498*, 94-98.

9 Gogineni, V.; Schinazi, R. F.; Hamann, M. T. Role of marine natural products in the genesis of antiviral agents. *Chem. Rev.* **2015,** *115*, 9655-9706.

10 Yu, Z.; Jing, H.; Pan, H. T.; Jia, F. R.; Jin, Y. T.; Xu, S. Y.; Venge, P. Distinction between bacterial and viral infections by serum measurement of human neutrophil lipocalin (HNL) and the impact of antibody selection. *J. Immunol. Methods* **2016,** *432*, 82-86.

11 Harbarth, S.; Balkhy, H. H.; Goossens, H.; Jarlier, V.; Kluytmans, J.; Laxminarayan, R.; Saam, M.; Van Belkum, A.; Pittet, D. Antimicrobial resistance: one world, one fight! *Antimicrob. Resist. Infect. Control.* **2015**, *4*, 49.

12 Gelband, H.; Miller-Petrie, M.; Pant, S.; Gandra, S.; Levinson, J.; Barter, D.; White, A.; Laxminarayan, R. The *State of the World's Antibiotics* **2015**. *https://cddep.org/publications/state_worlds_antibiotics_2015/*

13 Wenzel, B. The state of antibotics 2016. http://www.uspirg.org/blogs/blog/usp/state-antibiotics-2016.

14 Khachatourians, G. G. Agricultural use of antibiotics and the evolution and transfer of antibiotic-resistant bacteria. *Can. Med. Assoc. J.* **1998,** *159*, 1129-1136.

15 Tenover, F. C.; McGowan, J. E. Reasons for the emergence of antibiotic resistance. *Am. J. Med. Sci.* **1996,** *311*, 9-16.

16 Walsh, T. R.; Weeks, J.; Livermore, D. M.; Toleman, M. A. Dissemination of NDM-1 positive bacteria in the New Delhi environment and its implications for human health: an environmental point prevalence study. *Lancet. Infect. Dis.* **2011,** *11*, 355-362.

17 Kumarasamy, K. K.; Toleman, M. A.; Walsh, T. R.; Bagaria, J.; Butt, F.; Balakrishnan, R.; Chaudhary, U.; Doumith, M.; Giske, C. G.; Irfan, S.; Krishnan, P.; Kumar, A. V.; Maharjan, S.; Mushtaq, S.; Noorie, T.; Paterson, D. L.; Pearson, A.; Perry, C.; Pike, R.; Rao, B.; Ray, U.; Sarma, J. B.; Sharma, M.; Sheridan, E.; Thirunarayan, M. A.; Turton, J.; Upadhyay, S.; Warner, M.; Welfare, W.; Livermore, D. M.; Woodford, N. Emergence of a new antibiotic resistance mechanism in India, Pakistan, and the UK: a molecular, biological, and epidemiological study. *Lancet. Infect. Dis.* **2010,** *10*, 597-602.

18 Templeton, K. E.; Scheltinga, S. A.; Beersma, M. F. C.; Kroes, A. C. M.; Claas, E. C. J.

Rapid and sensitive method using multiplex real-time PCR for diagnosis of infections by influenza A and influenza B viruses, respiratory syncytial virus, and parainfluenza viruses 1, 2, 3, and 4. *J. Clin. Microbiol.* **2004,** *42*, 1564-1569.

19 van Elden, L. J. R.; van Kraaij, M. G. J.; Nijhuis, M.; Hendriksen, K. A. W.; Dekker, A. W.; Rozenberg-Arska, M.; van Loon, A. M. Polymerase chain reaction is more sensitive than viral culture and antigen testing for the detection of respiratory viruses in adults with hematological cancer and pneumonia. *Clin. Infect. Dis.* **2002,** *34*, 177-183.

20 Vanmilaan, A. J.; Sprenger, M. J. W.; Rothbarth, P. H.; Brandenburg, A. H.; Masurel, N.; Claas, E. C. J. Detection of respiratory syncytial virus by rna-polymerase chain-reaction and differentiation of subgroups with oligonucleotide probes. *J. Med. Virol.* **1994,** *44*, 80-87.

21 Zahraei, B.; Hashemzadeh, M. S.; Najarasl, M.; Zahiriyeganeh, S.; Tat, M.; Metanat, M.; Rad, N. S.; Khansari-nejad, B.; Zafari, E.; Sharti, M.; Dorostkar, R. Novel, in-house, SYBR green based one-step rRT-PCR: rapid and accurate diagnosis of crimean-congo hemorrhagic fever virus in suspected patients from Iran. *J. Microb.* **2016,** *9*, e57165.

22 Li, X. N.; Kong, H.; Mout, R.; Saha, K.; Moyano, D. F.; Robinson, S. M.; Rana, S.; Zhang, X. R.; Riley, M. A.; Rotello, V. M. Rapid identification of bacterial biofilms and biofilm wound models using a multichannel nanosensor. *ACS Nano* **2014,** *8*, 12014-12019.

23 Saha, K.; Agasti, S. S.; Kim, C.; Li, X. N.; Rotello, V. M. Gold nanoparticles in chemical and biological sensing. *Chem. Rev.* **2012,** *112*, 2739-2779.

24 Yuan, H. X.; Liu, Z.; Liu, L. B.; Lv, F. T.; Wang, Y. L.; Wang, S. Cationic conjugated polymers for discrimination of microbial pathogens. *Adv. Mater.* **2014,** *26*, 4333-4338.

25 Thomas, S. W.; Joly, G. D.; Swager, T. M. Chemical sensors based on amplifying fluorescent conjugated polymers. *Chem. Rev.* **2007,** *107*, 1339-1386.

26 Zhu, C. L.; Liu, L. B.; Yang, Q.; Lv, F. T.; Wang, S. Water-soluble conjugated polymers for imaging, diagnosis, and therapy. *Chem. Rev.* **2012,** *112*, 4687-4735.

27 Jurs, P. C.; Bakken, G. A.; McClelland, H. E. *Chem. Rev.* **2000**, 100, 2649-2678.

28 Xing, C. F.; Yang, G. M.; Liu, L. B.; Yang, Q.; Lv, F. T.; Wang, S. Conjugated polymers for light-activated antifungal activity. *Small* **2012**, *8*, 525-529.

29 Bai, H. T.; Chen, H.; Hu, R.; Li, M.; Lv, F. T.; Liu, L. B.; Wang, S. Supramolecular conjugated polymer materials for in situ pathogen detection. *ACS Appl. Mater. Interfaces* **2016**, *8*, 31550-31557.

30 Phillips, R. L.; Miranda, O. R.; You, C. C.; Rotello, V. M.; Bunz, U. H. F., Rapid and efficient identification of bacteria using gold-nanoparticle-Poly(para-phenyleneethynylene) constructs. *Angew. Chem. Int. Ed.* **2008**, *47*, 2590-2594.

31 Freeman, W. H. Biochemistry, Lubert Stryer, **1975**, p626-877.

32 Zhou, C. C.; Wang, F. Y.; Chen, H.; Li, M.; Qiao, F. L.; Liu, Z.; Hou, Y. B.; Wu, C. X.; Fan, Y. X.; Liu, L. B.; Wang, S.; Wang, Y. L. Selective antimicrobial activities and action mechanism of micelles self-assembled by cationic oligomeric surfactants. *ACS Appl. Mater. Interfaces* **2016,** *8*, 4242-4249.

33 Zhu, C. L.; Yang, Q.; Liu, L. B.; Wang, S. Visual optical discrimination and detection of microbial pathogens based on diverse interactions of conjugated polyelectrolytes with cells. *J. Mater. Chem.* **2011,** *21*, 7905-7912.

34 Zhu, C. L.; Yang, Q. O.; Liu, L. B.; Lv, F. T.; Li, S. Y.; Yang, G. Q.; Wang, S. Multifunctional cationic poly(p-phenylene vinylene) polyelectrolytes for selective recognition, imaging, and killing of bacteria over mammalian cells. *Adv. Mater.* **2011**, *23*, 4805-4810.

SYNOPSIS